[60]Fullerene-Peptides: Bio-Nano Conjugates with Structural and Chemical Diversity

Andrew R. Barron*

[1]*Department of Chemistry, Rice University, Houston, TX 77005, USA,* [2]*Department of Materials Science and Nanoengineering, Rice University, Houston, TX 77005, USA,* [3]*College of Engineering, Swansea University, Bay Campus, Swansea SA1 8QQ, Wales, UK,* [4]*Centre for Nanohealth, Swansea University, Singleton Park, Swansea SA2 8PP, Wales, UK.*

Corresponding author. E-mail: a.r.barron@swansea.ac.uk; arb@rice.edu

Keywords: C_{60}, amino acid, hydrophilic, HIV, cell, membrane

Fullerene-Peptides: Bio-Nano Conjugates with Structural and Chemical Diversity

[60]Fullerene-peptides represent a simple yet chemically diverse example of a bio-nano conjugate. The C_{60} provide the following attributes to the conjugate: a) precise three-dimensional architecture, b) a large hydrophobic mass, and c) unique electronic properties. Conversely, the peptide component provides: a) structural diversity depending on the overall length and amino acids composition, b) charge flexibility, and c) secondary structure and recognition. Recent advances in the synthetic strategy for [60]fullerene-peptide synthesis from both pre-formed peptides and using solid phase peptide synthesis (SPPS) are described. The effects of the hydrophobic C_{60} on the secondary structure of the peptide depend on the sequence of the latter, but in general the relative stability of particular structures is greatly enhanced. The ability of the [60]fullerene substituent to dramatically modify the both cellular uptake and transdermal transport is discussed as is the effects on cell viability and antimicrobial activity.

Introduction

The discovery of the first fullerene compound C_{60} is a pivotal moment in modern chemistry (1). Not only was it the discovery of a new form of elemental carbon, it also provided the archetype linkage between the molecular and nano regimes. No sooner was the discovery published than a plethora of researchers initiated studies of the physical and chemical properties of C_{60}, as well as its higher homologs (e.g., C_{70}), but also its elongated relatives (carbon nanotubes) (2). One feature of these materials that was quickly apparent was their extreme hydrophobic nature (3), which suggested limited biological implications due to the restricted transport in aqueous solution (4). However, it was this same hydrophobicity coupled with the electrochemical behaviour (5) that offered an interesting potential for interactions with biological systems (6,7,8).

Initial studies of the biological activity of fullerenes involved functionalization designed to enhance the solubility (7, 9), which involved chemical substituents with acid or basic groups to allow either the formation of charged species in water at relevant pH or enhanced hydrogen

bonding (10). A logical extension of this approach was the formation of zwitter ionic functionality, and it is here that amino acid moiety represents a flexible solution to solubility and functionality. The presence of potentially both positive ($-NH_3^+$) and negative ($-CO_2^-$) functionality offers compatibility in aqueous solutions over a range of pH and ionic concentration, while the inherent chemical functionality allows for their use as synthons to create larger structures. The first amino acid derivative of C_{60} was reported in 1993 (11), and since that time [60]fullerene amino acids have been prepared with a variety of linkage units (12-16). Figure 1 shows an idealized structure of a C_{60}-amino acid, where the linkage unit may or may not be either structurally related to a known amino acid, and can vary in its flexibility and length. The topic of [60]fullerene amino acids has been reviewed (17,18).

Given the composition of a peptide is a polymer of various amino acids, one obvious application of [60]fullerene-based amino acids is their incorporation into a peptide chain. The resulting [60]fullerene-peptide conjugate represents possibly the simplest, but chemically and structurally most flexible, bio-nano conjugate. The [60]fullerene moiety provides the following attributes to the conjugate: a) precise three-dimensional architecture, b) a large hydrophobic mass, and c) unique electronic properties (17). In contrast, the peptide component provides: a) structural diversity depending on the overall length and amino acids composition, b) charge flexibility, and c) secondary structure and recognition. There is also the potential that the presence of the hydrophobic [60]fullerene will modify the properties of the peptide and as such behavior unlike either of the component parts is possible.

The topic of [60]fullerene-peptide derivatives has been reviewed (17-20); however, recent results have shown the versatility of both synthetic methods and applications, and suggest that a fresh view is warranted.

Synthesis of C_{60}-peptide conjugates

Conceptually, there are two synthetic routes to the formation of [60]fullerene-peptide conjugates. The simplest is to functionalize [60]fullerene with a preformed peptide, while more challenging synthetically is to perform peptide synthesis where the [60]fullerene component is introduced as a non-natural amino acid in the peptide sequence.

Using a preformed peptide

The direct reaction of a suitably functionalized peptide chain with C_{60} was first reported by Romanova et al. (21). Using the high nucleophilicity of the primary amine in natural amino acids, reaction of C_{60} with various dipeptide derivatives (L-Ala-L-Ala, D,L-Ala-D,L-Ala, and Gly-L-Val) occurred via nucleophilic addition (Figure 2). As an alternative, Wang et al. (22) showed that methyl glycylglycinate (H-Gly_2-OMe) reacted via a nitrene intermediate (formed in the addition of Br_2) with C_{60} to form the dipeptide derivative (Figure 2). The use of a phase transfer overcame the issues associated with the low solubility of C_{60} in water.

The first [60]fullerene peptide was prepared by the reaction of a *N*-terminal free pentapeptide (Ala-Aib-Ala-Aib-Ala-OMe) with a methanofullerene through a linker based on a benzoic acid moiety (Figure 3) (23). Following this report a wide range of alternative linkage groups have been reported as being equally effective in facilitating the attachment of a preformed peptide (24-30). Much of this work has been subject to recent reviews (17-20), and a selection of the [60]fullerene derivatives used are also shown in Figure 3. One important route that was demonstrated with the immunomodulating peptide tuftsin (Thr-Lys-Pro-Arg) allowed for the covalent conjugate to be formed via either reaction with the amine or carboxylic acid termini (Figure 4), which provides a flexibility to attach further substituents.

Although it had been found that it is possible to insert a preformed [60]fullerene-amino acid into the center of a peptide during solid phase peptide synthesis (31), an alternative approach was reported, by Aroua et al., using a bis-*tert*-butyl ester (Figure 5) that was reacted

with resin-supported peptide to give a fulleropeptide (32). Of course the difference between this approach and that described below is that this method results in the same CO_2H termination at both ends of the resulting peptide. Thus, the latter may be better described as two peptides located on the same [60]fullerene.

Simultaneous peptide synthesis

With this route, the goal is to synthesis a [60]fullerene substituted amino acid that can react in a similar manner to any other amino acid and undergo polymerization, with other (naturally occurring) amino acids. In this manner, the [60]fullerene amino acid residue can be positioned at the end or within the resulting peptide chain. A further advantage of performing the reaction by solid phase peptide synthesis (SPPS) is that unlike solution phase methods, the purification process is much simpler. However, it is necessary to prepare C_{60}-derived amino acids suitable for subsequent reaction (14). Several suitable [60]fullerene derived amino acids have recently been reported, see Figure 6 (15,16,31,33).

The synthesis of a [60]fullerene peptide by SPPS was initially achieved using Fmoc (9-fluorenylmethoxycarbonyl protected) chemistry (14,34). The classical deprotection agent for the Fmoc protecting group is piperidine, and while it was initially reported that this was successful, subsequent work demonstrated that this result was erroneous as piperidine forms multiple stable adducts with the [60]fullerene core. To overcome this problem, it was suggested that 5% DBU (1,8-diazabicyclo[5.4.0]undec-7-ene) in DMF (dimethylformamide) was used for deprotection; however, great difficulty in obtaining a pure product even after HPLC purification results (35). It was shown that DBU interfers with mass spectrometry measurement and HPLC purification of the peptide. These difficulties led to the development of Boc (*tert*-butyloxycarbonyl) protecting group chemistry (31,36). It is interesting to note that the success of a particular coupling reaction (Boc versus Fmoc) must depend on the identity of the linkage group between the C_{60} and the amino acid, since the Fmoc chemistry was found to be successful

for Aza-C_{60}-Phe-OH (37), derived from the dipolar addition to C_{60} of the Fmoc-Nα-protected azido amino acids (16), but not for the [60]fullerene-substituted phenylalanine (Baa) prepared by cycloaddition (see Figure 6). It is unknown why an apparently small difference in the linkage group makes such a big difference in the reactivity.

In order to study how the presence and position within the peptide sequence of the [60]fullerene affects the structure and relative structural stability of the peptide's conformation, the sequences Glu-Ile-Ala-Gln-Leu-Glu-Tyr-Glu-Ile-Ser-Gln-Leu-Glu-Gln-NH_2 (2HP) was prepared in which either Baa (Figure 6) was added to the terminus (i.e., **Baa**-Glu-Ile-Ala-Gln-Leu-Glu-Tyr-Glu-Ile-Ser-Gln-Leu-Glu-Gln-NH_2) or tyrosine (Tyr) was replaced with Baa (i.e., Glu-Ile-Ala-Gln-Leu-Glu-**Baa**-Glu-Ile-Ser-Gln-Leu-Glu-Gln-NH_2). In addition, Baa was added to the terminus of Glu-Ile-Ala-Gln-Leu-Glu-Tyr-Glu-Ile-Ser-Gln-Leu-Glu-Gln-Glu-Ile-Gln-Ala-Leu-Glu-Ser-NH_2 (3HP) (i.e., **Baa**-Glu-Ile-Ala-Gln-Leu-Glu-Tyr-Glu-Ile-Ser-Gln-Leu-Glu-Gln-Glu-Ile-Gln-Ala-Leu-Glu-Ser-NH_2) (31). It was observed that the yield was lower and the purification more difficult when the [60]fullerene residue is within the sequence.

In addition to the facilitating of higher yields when the [60]fullerene derivative is at the end, rather than in the middle of the peptide sequence, it has also been observed that the further the [60]fullerene residue was placed from the polymer matrix solid support the higher the isolated yield, see Figure 7 (34). The overall length of the peptide chain also seems to play a role, as the recovery of the short peptides is difficult even when the [60]fullerene amino acid is inserted at the *N*-terminus. It has been suggested that the presence of the [60]fullerene affects the swelling properties of the polymeric solid support. In contrast, use of the *N*-Boc-Baa chemistry has been shown to result in high yields of the Baa-terminated peptides independent of the length of the peptide (31). However, the yield of the [60]fullerene peptide does show a dependence on the hydrophobicity of the peptide sequence: the more hydrophilic the sequence, the higher the yield (31).

One of the most interesting developments is the synthesis of an all [60]fullerene amino acid derived peptide by Watanabe et al. (35). Given the problems reported for solid phase synthesis due to the tendency of the [60]fullerene to become embedded onto the resin making it difficult to recover the product in reasonable yield (14,34) solution synthesis was used to prepare unique multi-[60]fullerene peptides. Coupling H-Gly-OBzl (Bzl = $CH_2C_6H_5$) to a functionalized [60]fullerene Fmoc-Af8-OH (Af8 = 2-amino-8-fulleropyrrolidinoalkanoic acid, see Figure 8a) followed by subsequent deprotection of the Fmoc group using 5% DBU in DMF resulted in the formation of *bis*-adduct of [60]fullerene. However, the use of the Boc method (using Boc-Af8-OH, Figure 8a) yielded Boc-Af8-Ala-OBzl. Deprotection of the Boc group with trifluoroacetic acid (TFA) allowed for coupling of the dipeptide benzyl ester with Boc-Af8-OH to give Boc-$(Af8)_2$-Ala-OBzl. Repetition of the deprotection and coupling steps gave the tetrapeptide Boc-$(Af8)_3$-Ala-OBzl (Figure 8b).

Finally an interesting footnote, since peptide biosynthesis offers a potential alternative to SPPS, the concept of creating an amino acylated 5'-phospho-2'-deoxyribocytidylribo-adenosine subunit containing a [60]fullerene amino acid (pdCpA-Baa) was attempted (37). Unfortunately, no reaction was observed between the hydrophilic phospho-cytidine-phospho-adenosine subunit (pdCpA) and hydrophobic Baa possibly due to the steric bulk of the latter.

Structural effects

The [60]fullerene containing peptides have been generally characterized by matrix assisted laser desorption/ionization (MALDI) mass spectrometry by the presence of the M^+, M^++H, or M^++Na ions, depending on the reaction conditions (31,36). In some cases the [60]fullerene-functionalized peptides are sufficiently soluble in H_2O to provide a UV-visible spectrum (36), while IR spectroscopy shows the functionalization of the C_{60} (39). However, it is the effect of the hydrophobic C_{60} moiety on the peptide configuration that is of most interest.

In the earliest report of [60]fullerene peptides it was shown that the presence of the [60]fullerene had a significant effect on the secondary structure of the peptide (34). Circular dichroism (CD) analysis of a peptide H-Gly-$(Nle)_2$-Gln-Orn-Nle-Gly-$(Orn)_2$-Nle-$(Orn)_2$-Nle-Gly-$(Orn)_2$-Nle-Gly-Tyr-NH_2 (Figure 9a) indicates indicated that it is unstructured in aqueous solution but assumes a partly helical structure (~40%) in the presence of the helix-promoting solvent, e.g., trifluoroethanol (TFE) or sodium dodecyl sulfate (SDS) (40). The shape of the CD spectra for fullero-peptides H-**Fgu**-Gly-$(Nle)_2$-Gln-Orn-Nle-Gly-$(Orn)_2$-Nle-$(Orn)_2$-Nle-Gly-$(Orn)_2$-Nle-Gly-Tyr-NH_2 and H-Gly-$(Nle)_2$-Gln-Orn-Nle-Gly-$(Orn)_2$-**Fgu**-$(Orn)_2$-Nle-Gly-$(Orn)_2$-Nle-Gly-Tyr-NH_2 (where Fgu = fulleropyrrolidino-glutamic acid, see Figure 6) instead indicates a significant degree of helix formation in aqueous solution (Figure 9b and c). Unlike the native peptide, the spectra for both fullero-peptides change distinctly in the presence of SDS micelles than of TFE (see Figure 9b and c). The shape of the spectrum for fullero-peptide H-Gly-$(Nle)_2$-Gln-Orn-Nle-Gly-$(Orn)_2$-**Fgu**-$(Orn)_2$-Nle-Gly-$(Orn)_2$-Nle-Gly-Tyr-NH_2 changes in a manner consistent with the presence of an extended conformation (34).

Although initial results suggested that the presence of a [60]fullerene substituent would change the relative stability of specific secondary structures, subsequent work showed that the [60]fullerene could either promote a different structure or preclude a structural change (31). For example while the parent peptide Glu-Ile-Ala-Gln-Leu-Glu-Tyr-Glu-Ile-Ser-Gln-Leu-Glu-Gln-NH_2 (2HP) adopts a random coil in aqueous solution, and is transformed via an α-helix to a β-sheet with decreasing pH, when the [60]fullerene amino acid Baa (Figure 6) is on the terminus (i.e., **Baa**-Glu-Ile-Ala-Gln-Leu-Glu-Tyr-Glu-Ile-Ser-Gln-Leu-Glu-Gln-NH_2) the β-sheet structure is observed at all pH values. In contrast, with the Baa in the middle of the peptide (i.e., Glu-Ile-Ala-Gln-Leu-Glu-**Baa**-Glu-Ile-Ser-Gln-Leu-Glu-Gln-NH_2) the random coil converts to an α-helix with decreasing pH, but never to a β-sheet (31). By contrast, the longer sequence **Baa**-Glu-Ile-Ala-Gln-Leu-Glu-Tyr-Glu-Ile-Ser-Gln-Leu-Glu-Gln-Glu-Ile-Gln-Ala-

Leu-Glu-Ser-NH_2 maintains an α-helix structure over all pH studied, while the parent is observed as a random coil in aqueous solution that converts to an α-helix with decreasing pH. It is thus clear that while the [60]fullerene has a significant effect of secondary structure there is no consistent effect, and further study will be important.

It has been observed that while [60]fullerene-peptides are soluble in water they form aggregates, presumably as a consequence of the presence of both hydrophobic (C_{60}) and hydrophilic (amino acid) groups within the same molecule (31). The relative size of the aggregates is found to depend on the pH of the solution, but independent of concentration. The [60]fullerene peptide Baa-Lys(FITC)-Lys_8-OH (FITC = fluorescein isothiocyanate) forms spherical and ellipsoidal cluster (average = 40-80 nm); however, upon addition of 10% SDS in PBS (phosphate-buffered saline), 100 nm diameter nano-tubule structures are formed, which in turn align to form bundles (Figure 10).

The self-assembling properties and morphology of [60]fullerene peptides of different chain lengths in comparison with the native amino acid have been studied using scanning electron microscopy (SEM) (29). Figure 11a shows a comparison of the self-organized structures of the tert-butyl ester of the parent [60]fullerene amino acid, Fp-GABA-O^{t}Bu (c.f. Figure 3, GABA = γ-aminobutyric acid) and the steroid derivative (Fp-GABA-OSt, Figure 11b) with those of the [60]fullerene peptidosteroid hybrids, Fp-GABA-Gly-GABA-OSt and Fp-GABA-GABA-Gly-GABA-OSt, Figure 11c and d, respectively. The shorter [60]fullerene peptidosteroid hybrid formed hierarchically organized, branched network of well-arranged rods (Figure 11c). Increasing the length of the peptide resulted in the formation of unordered slightly curled microsheets (Figure 11d). It was proposed that the supramolecular assembly is influenced by a balance between: 1) π-stacking interactions of the [60]fullerene moiety, 2) the hydrophobic interactions of the steroid unit, 3) the participation of the hydrogen bonding, and 4) van der Waals interactions associated with peptide chain and steroid moiety.

Antioxidant activity

The antioxidant activity C_{60} and its derivatives are well established, but low solubility and a tendency to aggregation are considered limiting factors of its application. The antioxidant assay of Baa (Figure 6) and the derived peptide, Baa-$(Glu)_4$-$(Gly)_3$-Ser-OH were determined in comparison with Trolox (6-hydroxy-2,5,7,8-tetramethylchroman-2-carboxylic acid), a commercially available potent antioxidant of the vitamin E family (31). As may be seen from Figure 12, the parent amino acid is a very potent antioxidant with an IC_{50} of 55.88 μM, i.e., about 10 times more potent than Trolox. The linear relation for the inhibition versus concentration is consistent with the electrochemical behavior of [60]fullerene amino acids showing the ability of the C_{60} core to accept multiple electrons (31). The IC_{50} of Baa-$(Glu)_4$-$(Gly)_3$-Ser-OH was determined to be 89 μM. It is unclear why there is a slight reduction in activity between Baa and the Baa-containing peptide. It is possible that aggregation of the Baa-peptide acts as a buffer limiting electron transfer processes. However, what was interesting was that [60]fullerene peptides with cationic sequences show no antioxidant activity.

In a different study, the antioxidant capacity was measured by the ferrous ion oxidation-xylenol orange (FOX) method for [60]fullerene peptidosteroid hybrids, Fp-GABA-Gly-GABA-OSt and Fp-GABA-GABA-Gly-GABA-OSt (Figure 11c and d, respectively) (29). As may be seen from Figure 13, there is significant improvement over vitamin C and C_{60} (29). This was suggested to be associated with reduced aggregation and high solubility of the peptide derivatives.

Cellular uptake

The incubation of human embryonic kidney (HEK-293) cells with Lys(FITC)-$(Lys)_8$-OH and Baa-Lys(FITC)-$(Lys)_8$-OH revealed that while the cationic peptide shows no ability to cross over the cell membrane, the addition of [60]fullerene amino acid (Baa, Figure 6) to the sequence

facilitates the intracellular localization of the peptide (36). A similar result is obtained for the non-fullerene phenylalanine substituted nuclear localization sequence (NLS) derivative (Phe-Lys(FITC)-$(Lys)_2$-Arg-Lys-Val-OH) that shows no uptake into HEK-293 cells, but Baa-Lys(FITC)-$(Lys)_2$-Arg-Lys-Val-OH not only exhibts uptake, but concentration in the nuclei of the cells (36). This results suggested that the presence of a nuclear localization sequence results in transport across the nuclear membrane. Neuroblastoma cells are known for their difficulty in transfection through the cell membrane. However, incubation of H-Baa-Lys(FITC)-$(Lys)_2$-Arg-Lys-Val-OH with human IMR-32 cells and treating with 4',6-diamidino-2-phenylindole (DAPI) nuclei staining dye (Figure 14) show intense point fluorescence in cytoplasm, and homogeneous intense fluorescence around nuclei closely associated with the blue of the DAPI nuclei staining dye. Additional studies showed that the uptake intensity for the anionic peptide Baa-Lys(FITC)-$(Glu)_4$-$(Gly)_3$-Ser is greatly reduced in comparison with the cationic [60]fullerene peptides of the same concentration. The cellular uptake is also decreased by the addition of increasing concentrations of γ-cyclodextrin (CD).

Given the ability of [60]fullerene-peptides to facilitate intra celluar transport (36), the mechanism of uptake of the poly-lysine derivative with a FITC label (Baa-Lys(FITC)-$(Lys)_8$-OH) was investigated (41). Baa-Lys(FITC)-$(Lys)_8$-OH was found to be present near the cell membrane at 15 min and entered into the cytoplasm by 30 min but did not localize in the lysosomes. Endocytic inhibitors showed that the endocytic pathways could be mediated by caveolae/lipid rafts and cytoskeletal components. A scavenger receptor inhibitor completely blocked the uptake of Baa-Lys(FITC)-$(Lys)_8$-OH, suggesting a specific endocytic pathway was strongly involved in Baa-Lys(FITC)-$(Lys)_8$-OH cellular uptake (41).

Toxicity and antimicrobial activity

The functionalization of C_{60} has the potential to provide greater interaction between the [60]fullerene and the biological environment yielding potential new medical and

pharmacological applications; however, there is equal concern over the potential toxicity of any such conjugate. Studies had shown that exposure of human epidermal keratinocytes (HEK) to the amino acid Baa (Figure 6) resulted in a decrease of the MTT cell viability after 48 h significantly decreased only for concentrations of >0.04 mg/mL (42). In addition, human cytokines IL-6, IL-8, TNF-α, IL-1b, and IL-10 were assessed, and indicated that at concentrations lower than 0.04 mg/mL cell viability is maintained.

Introduction of a [60]fullerene amino acid (Fgu, Figure 6) at the *N*-terminus of H-Gly-$(Nle)_2$-Gln-Orn-Nle-Gly-$(Orn)_2$-Nle-$(Orn)_2$-Nle-Gly-$(Orn)_2$-Nle-Gly-Tyr-NH_2 was shown to have a dramatic effect on both the antimicrobial activity of the peptide sequence (34). The activity is considerably reduced for *E. coli* and *C. albicans*, but increased for *S. aureus*, upon inclusion of the [60]fullerene. A similar behavior was observed for H-Gly-$(Nle)_2$-Gln-Orn-Nle-Gly-$(Orn)_2$-**Fgu**-$(Orn)_2$-Nle-Gly-$(Orn)_2$-Nle-Gly-Tyr-NH_2, where the [60]fullerene-based residue is positioned in the middle of the sequence. However, it was shown that the antimicrobial activity was most probably inherently due to the C_{60} rather than the specific sequence, since the fullero-peptide H-Gly-Orn-Gly-**Fgu**-Gly-Orn-Gly-NH_2 showed equal or better activity (34). The presence of C_{60} itself is clearly not totally a prerequisite for antimicrobial activity since, in a study of a series of [60]fullerene peptide derivatives, tested using the broth microdilution method against *Staphylococcus aureus* NCTC 6571 and *Escherichia coli* NCTC 10418, all the fullerenyl-based compounds were inactive, even at higher concentrations, with MIC greater than 100 to 340 (μg/mL) (28).

Possibly the result that is both disappointing and promising at the same time, is a study of a series of [60]fullerene-peptides, based upon Baa (Figure 6), with range of cell lines. Exposure of SH-SY5Y neuroblstoma cells to the Baa-peptides for 48 hrs showed no significant inhibition of cell growth by Baa-Lys(FITC)-Asn-Asp-Leu-Arg-Ser-**Ser-Phe-Leu**-Thr-Leu-Arg-Asp-His-Val (**Baa-1**) or Baa-Lys(FITC)-Asn-Asp-Leu-Arg-Ser-**Ser-Phe-Ala-** Thr-Leu-

Arg-Asp-His-Val (**Baa-2**) nor the parent peptides. However, whereas the peptide Phe-Lys(FITC)-Asn-Asp-Leu-Arg-Ser-**Ala-Phe-Ala**-Thr-Leu-Arg-Asp-His-Val showed no inhibition, the Baa derivative (Baa-Lys(FITC)-Asn-Asp-Leu-Arg-Ser-**Ala-Phe-Ala**-Thr-Leu-Arg-Asp-His-Val, **Baa-3**) showed significant inhibition towards this cell line at 40 μM. This initial result suggested that with the right combination of the [60]fullerene and the sequence controlled inhibition was possible (43).

A much more unexpected result was observed when the inhibitory effects of the Baa peptides and their parent peptides were tested against the proliferation of neuroblastoma cell lines IMR-32 and LAN-1 and breast cancer cell line MCF-7. While neither the parent peptides (Phe-Lys(FITC)-Asn-Asp-Leu-Arg-Ser-**Ser-Phe-Leu**-Thr-Leu-Arg-Asp-His-Val and Phe-Lys(FITC)-Asn-Asp-Leu-Arg-Ser-**Ala-Phe-Ala**-Thr-Leu-Arg-Asp-His-Val) showed significant inhibitory effects, their Baa peptide conjugate *activated* the proliferation of these cells (Figure 15). Although the underlying cause of this activation process was not explained (43), this effect if observed with other cell lines might constitute a possible therapeutic approach for degenerative illnesses where cell growth is haltered.

Antibody recognition

As noted in the introduction, one of the attributes of a peptide is its ability to be recognized. However, the question is whether the presence of a [60]fullerene disrupts or enhances this recognition? It is natural therefore to investigate whether an antibody would recognize an antigen peptide sequence when a [60]fullerene was present on the peptide.

Sofou et al. have reported the synthesis of a C_{60}-peptide (containing a solubilizing ethyleneglycol appendage) based upon the heptapeptide, H-$(Pro)_2$-Gly-Met-Arg-$(Pro)_2$-OH, which had been previously shown to have anti-genic properties (30). This proline-rich heptapeptide has been found to be the main target of the anti-Sm and anti-U1RNP autoantibodies in sera of patients with autoimmune diseases such as systemic lupus

erythematosus (SLE) and mixed connective tissue disease (MCTD). It was also found that the H-$(Pro)_2$-Gly-Met-Arg-$(Pro)_2$-OH epitope is recognized by anti-Ro/La positive sera, although they are negative for anti-Sm and anti-U1RNP (30). The [60]fullerene peptide (Figure 16), with oxidized methionine, was evaluated in comparison with the parent fulleropyrrolidine (Figure 3) for their ability to recognize anti-Sm and anti-U1RNP autoantibodies in SLE and MCTD patients' sera (ELISA experiment). In Table 1, the reactivities of the [60]fullerene peptide are listed in comparison with the parent peptide in its free and *C*-terminal amide form.

While the [60]fullerene-peptide strongly recognizes anti-Sm/U1RNP specificities, it was also recognized by anti-Ro/La positive sera, which are negative to anti-Sm/U1RNP sera. Most importantly, the parent [60]fullerene compound shows no recognition at all, suggesting that conversion of the carboxylic end of the parent peptide to an ester functionality in the [60]fullerene peptide was responsible for the decrease in disease specificity.

Enzymatic inhibition and anti-HIV activity

Immunomodulating peptide tuftsin (Thr-Lys-Pro-Arg) derivatives of C_{60} (Figure 11) were assayed for their stability against leucine aminopeptidase degradation and the immunostimulant activity to murine peritoneal macrophages were investigated *in vitro* (27). Compared with the natural tuftsin, both [60]fullerene derivatives showed significant enhancement of phagocytosis, chemotaxis activities and major histocompatibility complex class II (MHC II) molecule expression. The two conjugates also exhibit complete resistance to enzymatic hydrolysis, and were found to be non-toxic to macrophages in the tested concentrations. These results suggested that the C_{60}–tuftsin conjugates could be used as potential candidates of immune modulators and vaccine adjuvants (27).

The active site of the HIV-1 protease (HIV-1 PR) is a quasi-spherical hydrophobic cavity, whose diameter is about 10 Å. In a landmark paper Friedman et al., suggested from computer graphics simulation, that the hydrophobic cleft of HIV-1 protease could perfectly host

a C_{60} molecule (44). If the interaction between the C_{60} and HIV-1 PR could be made sufficiently strong, inhibition of the catalytic activity would be expected. However, the problem of solubilizing C_{60} in a medium suitable for biological tests was initially an issue since it is insoluble in water. Given the solubility of [60]fullerene-peptide conjugates it was suggested that these would be ideal candidates for HIV-1 inhibition (24).

Unfortunately, initial results were unpromising. Anti-HIV-1 protease activities were conducted on using a [60]fullerene conjugate of the pentapeptide sequence H-Thr-Thr-Asn-Tyr-Thr-OH (Figure 17), since this sequence is a known activator of human monocyte chemotaxis; however, the activity was shown to be moderate (K_i = 100 μM) (24). Some promise was given since the [60]fullerene-peptide activity was elevated compared to the underivatized peptide.

In an effort to narrow the plethora of possible "C_{60} fragment" and "peptide sequence" combinations an *in silico* drug screening approach was investigated (45). A database was created from a range of C_{60} derivatives and their binding scores with HIV-1 PR were computed using docking techniques, and compared with biological tests with purified HIV-1 PR. It was interesting that experimental results confirm the binding scores predicted from the docking calculations. From this data it was found that Fmoc-Baa (c.f. Figure 6) had about three times better inhibitory binding (K_i = 36 nM) than the most active [60]fullerene-based inhibitor (K_i = 103 nM) reported at that time (45). The calculations also suggested that the presence of the 9-fluorenylmethoxycarbonyl (Fmoc) protecting group on the [60]fullerene-substituted phenylalanine (i.e., Fmoc-Baa) improved the inhibition dramatically as compared to the corresponding free amino acid (Baa, Figure 6) because of a favorable interactions with the hydrophobic binding pocket (45). In order to determine if improved binding was possible through the incorporation of a designer peptide tail, a series of [60]fullerene amino acid derived peptides were prepared (37). In this case the terminal amino acid, Phe(4-aza-C_{60})-OH, was

derived from the dipolar addition to C_{60} of the Fmoc-Nα-protected azido amino acids derived from phenylalanine (16).

The rationale for the design of three peptide models was based on the structure of HIV-1 PR itself. It was hypothesized that an oligo-Lys peptide tail (Figure 18a) would provide both the positive charges and enough flexibility for the electrostatic interaction to occur (45). The knowledge that HIV-1 PR can recognize a Phe-Pro dipeptide subunit was the rationale for choosing a Pro-Hyp-Lys sequence (Figure 18b), and the Hyp-Hyp-Lys sequence (Figure 18c) was chosen because the addition of the second OH group present on Hyp (as compared to Pro) allows another opportunity for H-bonding (37). The position of the [60]fullerene peptides into the active site were determined *in silico* (Figure 19) and compared to the binding experimentally. The experimental results showed that all of the peptide derivatives showed improved inhibition over the C_{60} amino acid base; however, none were as effective as the most potent inhibitor reported previously, i.e., Fmoc-Baa-OH (45). The most active of the peptide inhibitors was Fmoc-Phe(4-aza-C_{60})-Hyp-Hyp-Lys-OH with two hydroxyproline residues (K_i = 76); which is much more active than Fmoc-Phe(4-aza-C_{60})-Pro-Hyp-Lys-OH (K_i = 120), with only one hydroxyproline residue. It is unknown if the observed increase in binding affinity was due to better placement of the second hydroxyl moiety in regards to the aspartyl residues or if it is was due to the increase in H-bonding opportunities; however the difference in energy is worth approximately that of a H-bond.

Recent quantitative structure–activity relationship models (QSAR) and docking calculations have shown that [60]fullerene derivative with two O atoms and an additional hydroxymethylcarbonyl (HMC) group has good HIV-1 protease inhibitory properties (46). The resulting balance between hydrophobic and hydrogen bonding was discussed, and in combination with the results observed for the [60]fullerene-peptides should guide the future direction of this research.

Transdermal effects

The ability of nanomaterials (such as quantum dots and fullerenes) to penetrate intact skin (47,48) can be either a concern with regard to toxicity or provide a route for drug delivery. Given that the addition of a [60]fullerene-derived amino acid to a cationic peptide results in the peptide showing cellular uptake, whereas the same peptide sequence in the absence of Baa shows no transport across the cell membrane (36), it was logical to investigate whether the same [60]fullerene-peptides could facilitate transdermal transport. Dermatomed porcine skin was fixed to a flexing device and topically dosed with an aqueous solution of a [60]fullerene-substituted phenylalanine (Baa, Figure 6) derivative of a nuclear localization peptide sequence, Baa-Lys(FITC)-NLS (NLS = Pro-Lys-Lys-Lys-Arg-Lys-Val) (49). The skin was flexed or left unflexed (control) and confocal microscopy demonstrated that dermal penetration of the nanoparticles at 8 h in skin flexed for at least 60 min (Figure 20). In contrast, Baa-Lys-(FITC)-NLS did not penetrate into the dermis of unflexed skin until 24 h. Thus, flexing has a significant effect on the uptake.

Although the mechanisms by which the flexing increases nanoparticle penetration was not determined, dynamic light scattering (DLS) and transmission electron microscopy (TEM) analyses found that in solution Baa-Lys(FITC)-NLS forms spherical and ellipsoidal clusters with average aggregate sizes of approximately 40-250 nm. Given that the vertical and lateral gaps between corneocytes present in the stratum corneum are about 19 nm (50) it suggested that the Baa-Lys(FITC)-NLS aggregates would be unlikely to diffuse through the epidermal layers via intercellular spaces. It is evident from the results of this study, however, that the [60]fullerene-based peptides do penetrate through the epidermal layers via passive diffusion and that flexing increases this penetration. TEM analysis revealed [60]fullerene-peptide localization within the intercellular spaces of the stratum granulosum. Clearly, further studies of the effects of different peptide sequences would be necessary in order to create a better

understanding of the mechanism of transdermal transport.

Conclusions

The recent work on [60]fullerene-peptides has shown their potential application across a wide range of applications. Some of these are expected, such as their antioxidant properties. However, the ability of the C_{60} moiety to facilitate cellular uptake and transdermal transport where the analogous parent peptides show no propensity, demonstrates the new chemistry observed for the conjugate as compared to the components. The understanding of the effects of such a compact superhydrophobic moiety within a biological system is only now being explored, and the use of computer simulation offers a real opportunity to screen many possible structures.

Declaration of interest

This work was supported by the Robert A. Welch Foundation (C-0002), the Welsh Government Sêr Cymru Programme, and the National Academies Keck Futures Initiative. The author declares no competing financial interests.

References

(1) Kroto HW, Heath JR, O'Brien SC, Curl RF, Smalley RE. C_{60}: Buckminsterfullerene. Nature 1985;318:162-163.

(2) Dresselhaus MS, Dresselhaus G, Eklund PC. Science of Fullerenes and Carbon Nanotubes: Their Properties and Applications. Cambridge: Academic Press, 1996.

(3) Zichi DA, Rossky PJ. Solvent molecular dynamics in regions of hydrophobic hydration. J Chem Phys 1986;84:2814-2822.

(4) Lecoanet HF, Bottero J-Y, Wiesner MR. Laboratory assessment of the mobility of nanomaterials in porous media. Environ Sci Technol 2004;38, 5164-5169.

(5) Yang Y, Arias F, Echegoyen L, Chibante LPF, Flanagan S, Robertson A, Wilson LJ. Reversible fullerene electrochemistry: correlation with the HOMO-LUMO energy difference for C_{60}, C_{70}, C_{76}, C_{78}, and C_{84}. J Am Chem Soc 1995;117:7801-7804.

(6) Bosi S, Da Ros T, Spalluto G, Prato M. Fullerene derivatives: an attractive tool for biological applications. Euro J Med Chem 2003;38:913-923.

(7) Jensen W, Wilson SR, Schuster DI. Biological applications of fullerenes. Bioog Med Chem 1996;4:767-779.

(8) Bakry R, Vallant RM, Najam-ul-Haq M, Rainer M, Szabo Z, Huck CW, Bonn GK. Medicinal applications of fullerenes. Int J Nanomedicine 2007;2:639-649.

(9) Djordjevic A, Srdjenovic B, Seke M, Petrovic D, Injac R, Mrdjanovic J. Review of synthesis and antioxidant potential of fullerenol nanoparticles. J Nanomater 2015;2015: 567073.

(10) Sun Y-P, Lawson GE, Huang W, Wright AD, Moton DK. Preparation and characterization of highly water-soluble pendant fullerene polymers. Macromolecules 1999;32:8747-8752.

(11) An Y-Z, Anderson JL, Rubin Y. Synthesis of α-amino acid derivatives of C_{60} from 1,9-(4-hydroxycyclohexano)buckminsterfullerene. J Org Chem 1993;58:4799-4801.

(12) Skiebe A, Hirsch A. A facile method for the synthesis of amino acid and amido derivatives of C_{60}. J Chem Soc Chem Commun 1994;335-336.

(13) Gan L, Zhou D, Luo C, Tan H, Huang C, Lu M, Pan J, Wu Y. Synthesis of fullerene amino acid derivatives by direct interaction of amino acid ester with C_{60}. J Org Chem 1996;61:1954-1961.

(14) Pellarini F, Pantarotto D, Da Ros T, Giangaspero A, Tossi A, Prato M. A novel [60]fullerene amino acid for use in solid-phase peptide synthesis. Org Lett 2001;3:1845-1848.

(15) Yang J, Barron AR. A new route to fullerene substituted phenylalanine derivatives. Chem Commun 2004:2884-2885.

(16) Strom TA, Barron AR, A simple quick route to fullerene amino acid derivatives. Chem Commun 2010:4764-4766.

(17) Burley GA, Keller PA, Pyne SG. [60]Fullerene amino acids and related derivatives. Fullerene Sci Techn 1999;7:973-1001.

(18) Bianco A, da Ros T, Prato M, Toniolo C. Fullerene-based amino acids and peptides. J Peptide Sci 2001;7:208-219

(19) Pantarotto D, Tagmatarchis N, Bianco A, Prato M. Synthesis and biological properties of fullerene-containing amino acids and peptides. Mini Rev Med Chem 2004;4:805-814.

(20) Jennepalli S, Pyne SG, Keller PA. [60]Fullerenyl amino acids and peptides: a review of their synthesis and applications. RSC Adv 2014;4:46383-46398.

(21) Romanova VS, Tsyryapkin VA, Lyakhovetsky YI, Parnes ZN, Vol'pin ME. Addition of amino acids and dipeptides to fullerene C_{60} giving rise to monoadducts. Russ Chem Bull 1994;43:1090-1091.

(22) Wang N, Li J, Zhu D, Chan TH. A C_{60}-derivatized dipeptide. Tetrahedron Lett 1995;36:431–434.

(23) Prato M, Bianco A, Maggini M, Scorrano G, Toniolo C, Wudl F. Synthesis and characterization of the first fullerene-peptide. J Org Chem 1993;58:5578–5580.

(24) Toniolo C, Bianco A, Maggini M, Scorrano G, Prato M, Marastoni M, Tomatis R, Spisani S, Palu G, Blair ED. A bioactive fullerene peptide. J Med Chem 1994;37:4558-4562.

(25) Bianco A, Bertolini T, Crisma M, Valle G, Toniolo C, Maggini M, Scorrano G, Prato M. i-Turn induction by C_{60}-based fulleroproline: synthesis and conformational characterization of Fpr/Pro small peptides. J Peptide Sci 1997;50:159–170.

(26) Bianco A, Maggini M, Scorrano G, Toniolo C, Marconi G, Villani C, Prato M. Synthesis, chiroptical properties, and configurational assignment of fulleroproline derivatives and peptides. J Am Chem Soc 1996;118:4072-4080.

(27) Xu Y, Zhu J, Xiang K, Li Y, Sun R, Ma J, Sun H, Liu Y, Synthesis and immunomodulatory activity of [60]fullerene–tuftsin conjugates. Biomaterials 2011;32:9940-9949.

(28) Jennepalli S, Hammer KA, Riley TV, Pyne SG, Keller PA. Synthesis of mono and bis[60]fullerene-based dicationic peptoids. Eur J Org Chem 2015;2015:195-201.

(29) Bjelaković MS, Kop TJ, Vlajić M, Đorđević J, Milić DR, Design, synthesis, and characterization of fullerene-peptide-steroid covalent hybrids. Tetrahedron 2014;70:8564-8570.

(30) Sofou P, Elemes Y, Panou-Pomonis E, Stavrakoudis A, Tsikaris V, Sakarellos C, Sakarellos-Daitsiotis M, Maggini M, Formaggio F, Toniolo C. Synthesis of a proline-rich [60]fullerene peptide with potential biological activity. Tetrahedron 2004;60:2823-2828.

(31) Yang Y, Alemany LB, Driver J, Hartgerink JD, Barron AR. Fullerene-derivatized amino acids: synthesis, characterization, antioxidant properties, and solid phase peptide synthesis. Chem Eur J 2007;3:2530-2545.

(32) Aroua S, Schweizer WB, Yamakoshi Y. C_{60} Pyrrolidine bis-carboxylic acid derivative as a versatile precursor for biocompatible fullerenes. Org Lett 2014;16:1688-1691.

(33) Innocenti A, Durdagi S, Doostdar N, Strom TA, Barron AR, Supuran CT. Nanoscale enzyme inhibitors: fullerenes inhibit carbonic anhydrase by occluding the active site entrance. Biorg Med Chem 2010;18:2822-2828.

(34) Pantarotto D, Bianco A, Pellarini F, Tossi A, Giangaspero A, Zelezetsky I, Briand JP, Prato M. Solid-phase synthesis of fullerene-peptides. J Am Chem Soc 2002;124:12543-12549.

(35) Watanabe LA, Bhuiyan MPI, Jose B, Kato T, Nishino N. Synthesis of novel fullerene amino acids and their multifullerene peptides. Tetrahedron Letters, 2004;45:7137-7140.

(36) Yang J, Wang K, Driver J, Yang J, Barron AR. The use of fullerene substituted phenylalanine derivatives as a passport through cell membranes. Org Biomol Chem 2007;5:260-266.

(37) Strom TA, Durdagi S, Ersoz SS, Salmas RE, Supuran CT, Barron AR, Fullerene-based inhibitors of HIV-1 protease. J Peptide Sci 2015;21:862-870.

(38) Strom TA, Barron AR. Attempts towards the bucky-amino acid acylation of the phospho-cytidine-phospho-adenosine (pdCpA) subunit. All Res J Nano 2015;1:4-9.

(39) Klemenkova ZS, Romanova VS, Tsyryapkin VA, Muradan VE, Parnes ZN, Lokshin BV, Vol'pin ME. Infrared spectra of amino acid and peptide monoderivatives of [60]fullerene and their methyl esters. Mendeleev Commun 1996;6:60-62.

(40) Pacor S, Giangaspero A, Bacac M, Sava G, Tossi A. Analysis of the cytotoxicity of synthetic antimicrobial peptides on mouse leucocytes: implications for systemic use. J Antimicrob Chemother 2002;50:339-348.

(41) Zhang LW, Yang J, Barron AR, Monteiro-Riviere NA. Endocytic mechanisms and toxicity of a functionalized fullerene in human cells. Tox Lett 2009;191:149-157.

(42) Rouse JG, Yang J, Barron AR, Monteiro-Riviere NA. Fullerene-based amino acid interactions with human epidermal keratinocytes, Toxicol in Vitro 2006;20:1313-1320.

(43) Doostdar N, In-vitro model system for calcific band keratopathy and inhibitory effects of C_{60} fullerene derivatives, PhD Thesis, Rice University (2010).

(44) Friedman SH, De Camp DL, Sijbesma RP, Srdanov G, Wudl F, Kenyon GL. Inhibition of the HIV-1 protease by fullerene derivatives: model building studies and experimental verification. J Am Chem Soc 1993;115:6506-6509.

(45) Durdagi S, Supuran CT, Strom TA, Doostdar N, Kumar MK, Barron AR, Mavromoustakos T, Papadopoulos MG. *In silico* drug screening approach to designing magic bullets: A successful example with anti-HIV fullerene derivatized amino acids. J Chem Inf Model 2009;49:1139-1143.

(46) Saleh NA. The QSAR and docking calculations of fullerene derivatives as HIV-1 protease inhibitors Spectrochim Acta A Mol Biomol Spectrosc 2015;136:1523-1529.

(47) Ryman-Rasmussen JP, Riviere JE, Monteiro-Riviere NA. Penetration of intact skin by quantum dots with diverse physicochemical properties. Toxicol Sci 2006;91:159-165.

(48) Prow TW, Monteiro-Riviere NA, Inman AO. Grice JE, Chen X, Zhao X, Sanchez WH, Gierden A, Kendall MA, Zvyagin AV, Erdmann D, Riviere JE, Roberts MS. Quantum dot penetration into viable human skin. Nanotoxicology 2012;6:173-185.

(49) Rouse JG, Ryman-Rasmussen JP, Yang J, Barron AR, Monteiro-Riviere NA, Effects of mechanical flexion on the penetration of fullerene amino acid-derivatized peptide nanoparticles through skin. Nano Lett 2007;7:155-160.

(50) van der Merwe D, Brooks JD, Gehring R, Baynes RE, Monteiro-Riviere NA, Riviere JE. A physiologically based pharmacokinetic model of organophosphate dermal absorption. Toxicol Sci 2006;89:188-204.

Table 1. Reactivity of sera containing various auto-antibodies (30).

Derivative	Anti-Sm/U1RNP (+) anti-Ro/La (-) (%)	Anti-Ro/La (+) anti-Sm/U1RNP (-) (%)
H-PPGMRPP-OH	75	40
H-PPGMRPP-NH_2	75	17
Fullero-peptide [a]	92	100
Fullero-pyrrolidine [b]	0	0

[a] See Figure 16. [b] See Figure 3.

Figure captions

Figure 1. A schematic representation of an idealized [60]fullerene amino acid.

Figure 2. Synthesis of C_{60}-dipeptide conjugates via either nucleophilic addition or a nitrene intermediate (21,22).

Figure 3. [60]fullerene derivatives used for the attachment of a preformed peptide.

Figure 4. Two routes to the C_{60} conjugate with the immunemodulating peptide tuftsin (Thr-Lys-Pro-Arg), yielding (a) NH_2–tuftsin–C_{60} and (b) C_{60}–tuftsin–CO_2H (27). Boc = tert-butyloxycarbonyl, Pbf = 2,2,4,6,7-pentamethyl-2,3-dihydrobenzofuran-5-sulfonyl, EDC = 1-ethyl-3-(3-dimethylaminopropyl) carbodiimide, HOBT = 1-hydroxybenzo-triazole, DIEA = diisopropylethylamine, DMF = dimethyl sulfoxide, DCM = dichloromethane, TFA = trifluoroacetic acid, TIS = triisopropylsilane, HBTU = O-benzotriazole-N,N,N′,N′-tetramethyl-uronium-hexafluoro-phosphate, DBU = 1,8-diazabicyclo[5,4,0]undecen-7-ene.

Figure 5. Reaction of *bis*-carboxylic acid [60]fullerene derivative with resin supported peptide, NH_2-GABA-GPLGVRGA-CO_2-resin (GABA = γ-aminobutyric acid) to provide a fulleropeptide (32).

Figure 6. Selection of [60]fullerene amino acid derivatives.

Figure 7. Plot of the recovered yield of crude peptide in the cleavage step as a function of the distance of the [60]fullerene-based residue (Fgu = fulleropyrrolidino-glutamic acid, see Figure

6) from the resin. Data from reference 34.

Figure 8. The [60]fullerene Fmoc-Af8-OH (Af8 = 2-amino-8-fulleropyrrolidinoalkanoic acid (a) and a computer model of tetrapeptide Boc-$(Af8)_3$-Ala-OBzl (b). Adapted with permission from Watanabe LA, Bhuiyan MPI, Jose B, Kato T, Nishino N. Synthesis of novel [60]fullerene amino acids and their multi-[60]fullerene peptides. Tetrahedron Letters, 2004;45:7137-7140. Copyright (2004) Elsevier Ltd.

Figure 9. CD spectra of peptide H-Gly-$(Nle)_2$-Gln-Orn-Nle-Gly-$(Orn)_2$-Nle-$(Orn)_2$-Nle-Gly-$(Orn)_2$-Nle-Gly-Tyr-NH_2 (a) and the corresponding fullero-peptides H-**Fgu**-Gly-$(Nle)_2$-Gln-Orn-Nle-Gly-$(Orn)_2$-Nle-$(Orn)_2$-Nle-Gly-$(Orn)_2$-Nle-Gly-Tyr-NH_2 (b) and H-Gly-$(Nle)_2$-Gln-Orn-Nle-Gly-$(Orn)_2$-**Fgu**-$(Orn)_2$-Nle-Gly-$(Orn)_2$-Nle-Gly-Tyr-NH_2 (c) at 4×10^{-5} M concentration, in aqueous 5 mM phosphate buffer (pH 7) (···) or in the presence of 50% TFE (–··–) or 10 mM SDS (s) in phosphate buffer (---). Fgu = fulleropyrrolidino-glutamic acid, see Figure 6. Reprinted with permission from Pantarotto D, Bianco A, Pellarini F, Tossi A, Giangaspero A, Zelezetsky I, Briand JP, Prato M. Solid-phase synthesis of [60]fullerene-peptides. J Am Chem Soc 2002;124:12543-12549. Copyright (2002) American Chemical Society.

Figure 10. TEM micrographs of the aggregates formed by Baa-Lys(FITC)-Lys_8-OH (a) in PBS buffer (1 $mg.mL^{-1}$ @ pH=7) and (b) with 10% SDS in PBS buffer. Scale bars = 200 and 50 nm, respectively. Adapted with permission from Yang Y, Alemany LB, Driver J, Hartgerink JD, Barron AR. Fullerene-derivatized amino acids: synthesis, characterization, antioxidant properties, and solid phase peptide synthesis. Chem Eur J 2007;3:2530-2545. Copyright (2007) Wiley-VCH Verlag Gmbh & Co.

Figure 11. SEM images of the self-organized structures of (a) Fp-GABA-O^{t}Bu, (b) Fp-GABA-OSt and [60]fullerene peptidosteroid hybrids (c) Fp-GABA-Gly-GABA-OSt and (d) Fp-GABA-GABA-Gly-GABA-OSt, upon evaporation from a 9:1 PhMe/MeOH mixture deposited on glass substrate at room temperature and their 3D-structures. Scale bars correspond to 5 μm. Reproduced with permission from Bjelaković MS, Kop TJ, Vlajić M, Đorđević J, Milić DR, Design, synthesis, and characterization of fullerene-peptide-steroid covalent hybrids. Tetrahedron 2014;70:8564-8570. Copyright (2014) Elsevier Ltd.

Figure 12. Plot of inhibition (%) as a function of reagent concentration for antioxidant activity comparison using (a) Baa, (b) Baa-$(Glu)_4$-$(Gly)_3$-Ser-OH, and (c) Trolox. Adapted with permission from Yang Y, Alemany LB, Driver J, Hartgerink JD, Barron AR. Fullerene-derivatized amino acids: synthesis, characterization, antioxidant properties, and solid phase peptide synthesis. Chem Eur J 2007;3:2530-2545. Copyright (2007) Wiley-VCH Verlag Gmbh & Co.

Figure 13. Comparison of the antioxidant capacities of Fp-GABA-Gly-GABA-OSt and Fp-GABA-GABA-Gly-GABA-OSt (Figure 11c and d, respectively) with regard to vitamin C and C_{60} measured by FOX assay. Adapted with permission from Bjelaković MS, Kop TJ, Vlajić M, Đorđević J, Milić DR, Design, synthesis, and characterization of fullerene-peptide-steroid covalent hybrids. Tetrahedron 2014;70:8564-8570. Copyright (2014) Elsevier Ltd.

Figure 14. Fluorescence micrographs of neuroblastoma cells incubated with (green) Baa-Lys(FITC)-$(Lys)_2$-Arg-Lys-Val-OH and (blue) DAPI. Scale bar = 150 μm. Reproduced with permission from Yang J, Wang K, Driver J, Yang J, Barron AR. The use of fullerene substituted

phenylalanine derivatives as a passport through cell membranes. Org Biomol Chem 2007;5:260-266. Copyright (2007) Royal Society of Chemistry.

Figure 15. Cell line proliferation for neuroblastoma cell lines (a) IMR-32 and (b) LAN-1, and (c) breast cancer cell line MCF-7 in the presence of DMSO (red), Baa-Lys(FITC)-Asn-Asp-Leu-Arg-Ser-**Ser-Phe-Leu**-Thr-Leu-Arg-Asp-His-Val (Baa-1) (blue) and Baa-Lys(FITC)-Asn-Asp-Leu-Arg-Ser-**Ala-Phe-Ala**-Thr-Leu-Arg-Asp-His-Val (yellow) (43).

Figure 16. Structure of [60]fullereo-peptide with oxidized methionine (30)

Figure 17. Structure of [60]fullerene derivative of the of the pentapeptide sequence H-Thr-Thr-Asn-Tyr-Thr-OH (24).

Figure 18. Structure of the C_{60}-amino acid-based peptides synthesized and used in the HIV-1 PR inhibition study (37).

Figure 19. IFD position of Fmoc-Phe(4-aza-C_{60})-Lys_3-OH into the HIV-1 PR active site. Dashed blue lines indicate H-bonds. Reproduced with permission Strom TA, Durdagi S, Ersoz SS, Salmas RE, Supuran CT, Barron AR, Fullerene-based inhibitors of HIV-1 protease. J Peptide Sci 2015;21:862-870. Copyright (2015) John Wiley & Sons, Ltd.

Figure 20. Confocal scanning microscopy images of intact skin dosed with Baa-Lys(FITC)NLS for 8 h (FITC = fluorescein isothiocyanate; NLS = Pro-Lys-Lys-Lys-Arg-Lys-Val). Top row: confocal-differential interference contrast (DIC) channel image shows an intact stratum corneum (SC) and underlying epidermal (E) and dermal layers (D). Middle row: Baa-

Lys(FITC)-NLS fluorescence channel (green) and confocal-DIC channel show [60]fullerene penetration through the epidermal and dermal layers of skin. Bottom row: fluorescence intensity scan showing Baa-Lys(FITC)-NLS penetration. All scale bars represent 50 μm. Reproduced with permission from Rouse JG, Ryman-Rasmussen JP, Yang J, Barron AR, Monteiro-Riviere NA, Effects of mechanical flexion on the penetration of fullerene amino acid-derivatized peptide nanoparticles through skin. Nano Lett 2007;7:155-160. Copyright (2007) American Chemical Society.

Fig. 1.

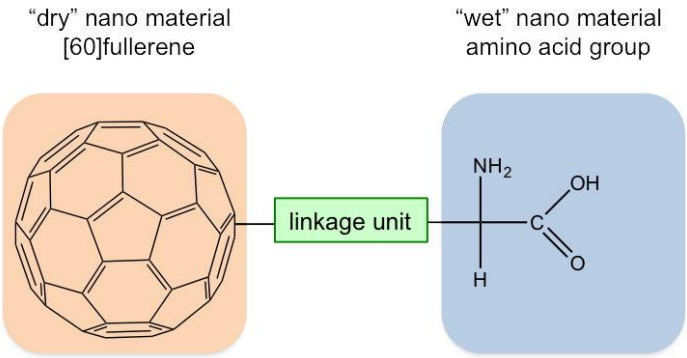
“dry” nano material
[60]fullerene
“wet” nano material
amino acid group
linkage unit
NH2
OH
C
O
H

Fig. 2.

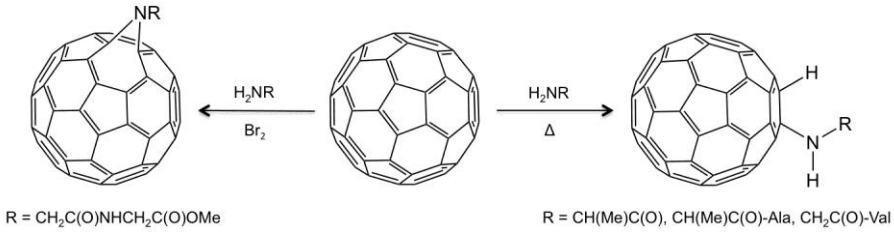
NR
H2NR
Br2
H2NR
Δ
H
N
H
R
R = CH2C(O)NHCH2C(O)OMe
R = CH(Me)C(O), CH(Me)C(O)-Ala, CH2C(O)-Val

Fig. 3.

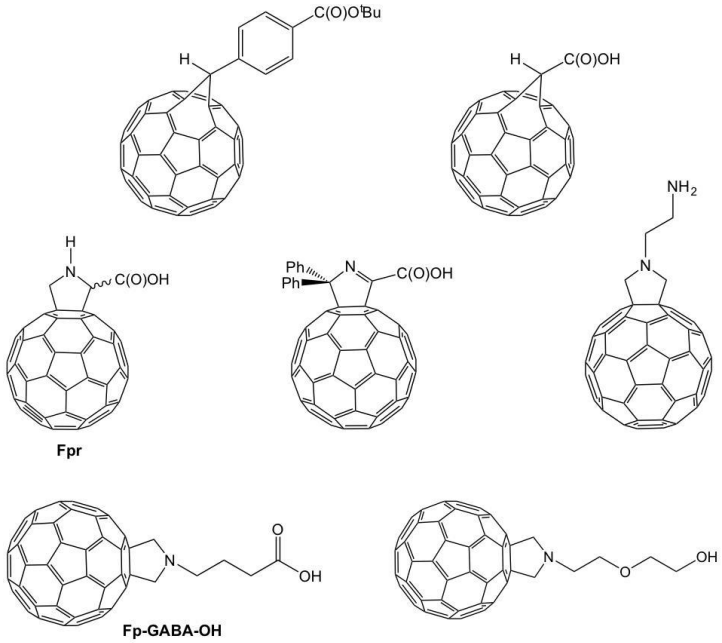

Fig. 4.

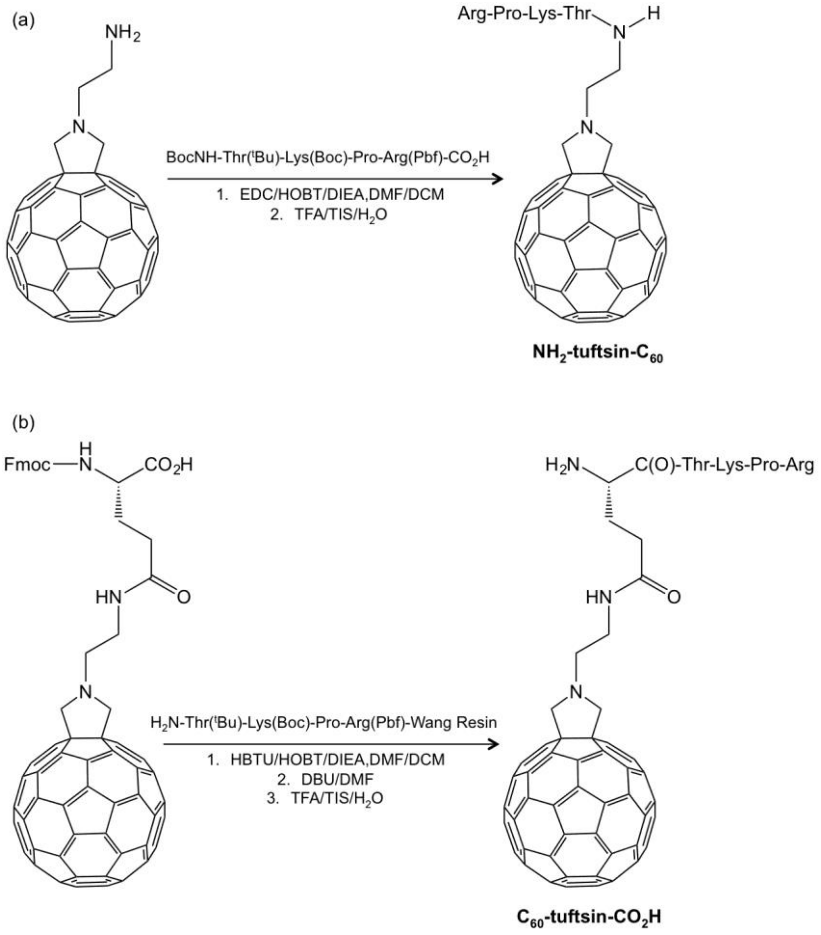
(a)
NH2
N
BocNH-Thr(tBu)-Lys(Boc)-Pro-Arg(Pbf)-CO2H
1. EDC/HOBT/DIEA,DMF/DCM
2. TFA/TIS/H2O
Arg-Pro-Lys-Thr
N
H
N
NH2-tuftsin-C60
(b)
Fmoc
H
N
CO2H
HN
O
N
H2N-Thr(tBu)-Lys(Boc)-Pro-Arg(Pbf)-Wang Resin
1. HBTU/HOBT/DIEA,DMF/DCM
2. DBU/DMF
3. TFA/TIS/H2O
H2N
C(O)-Thr-Lys-Pro-Arg
HN
O
N
C60-tuftsin-CO2H

Fig. 5.

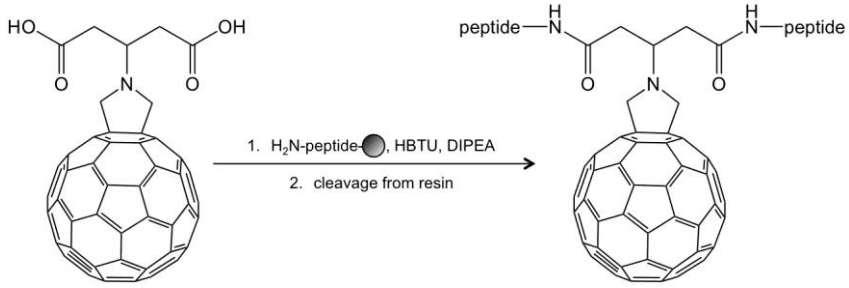
HO
OH
O
N
O
peptide—N
H
N—peptide
1. H2N-peptide-resin, HBTU, DIPEA
2. cleavage from resin

Fig. 6.

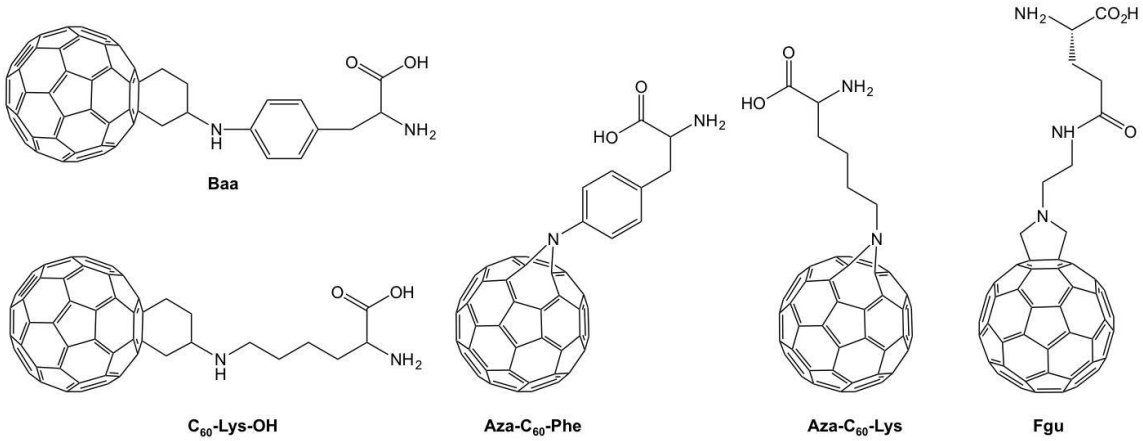

Fig. 7.

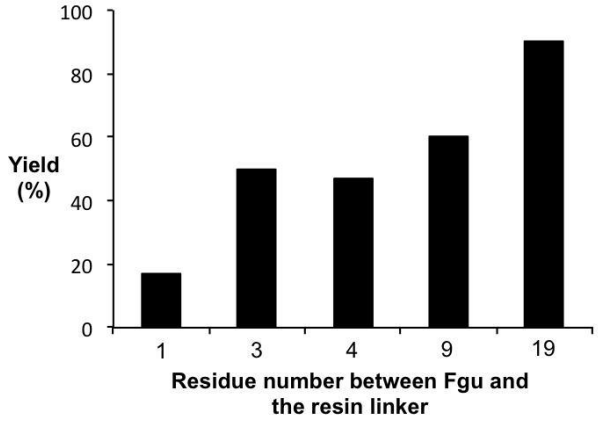
100
80
60
40
20
0
Yield (%)
1
3
4
9
19
Residue number between Fgu and the resin linker

Fig. 8.

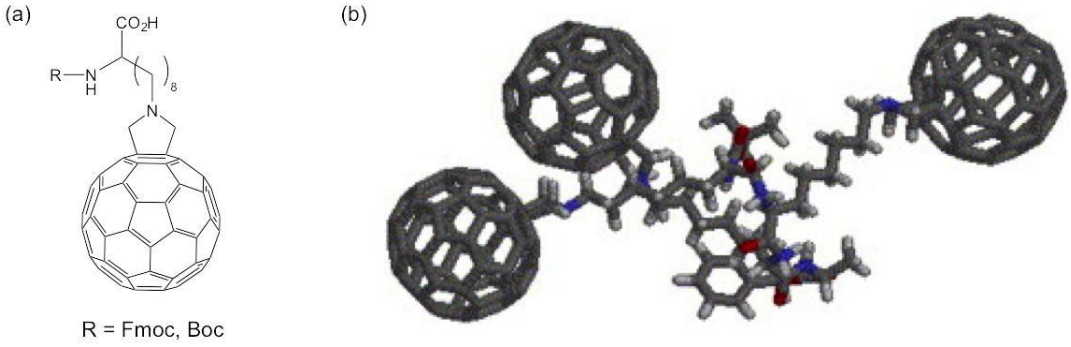

Fig. 9.

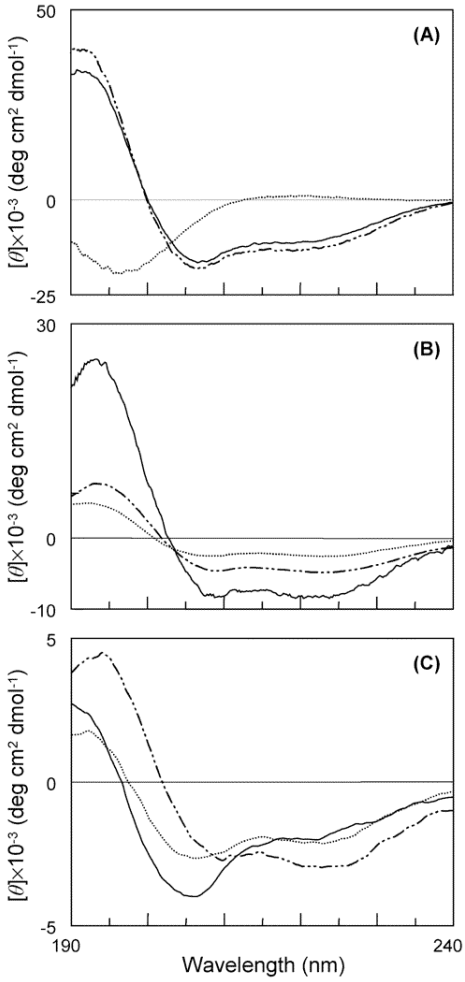

Fig. 10.

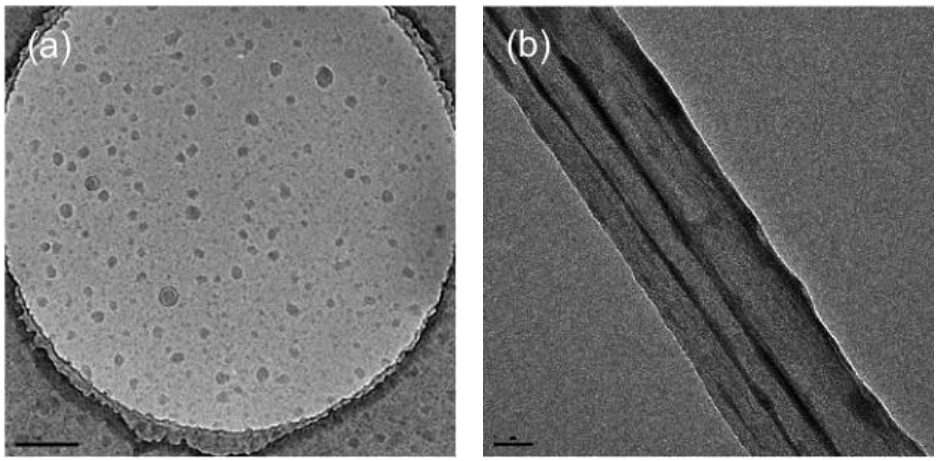

Fig. 11.

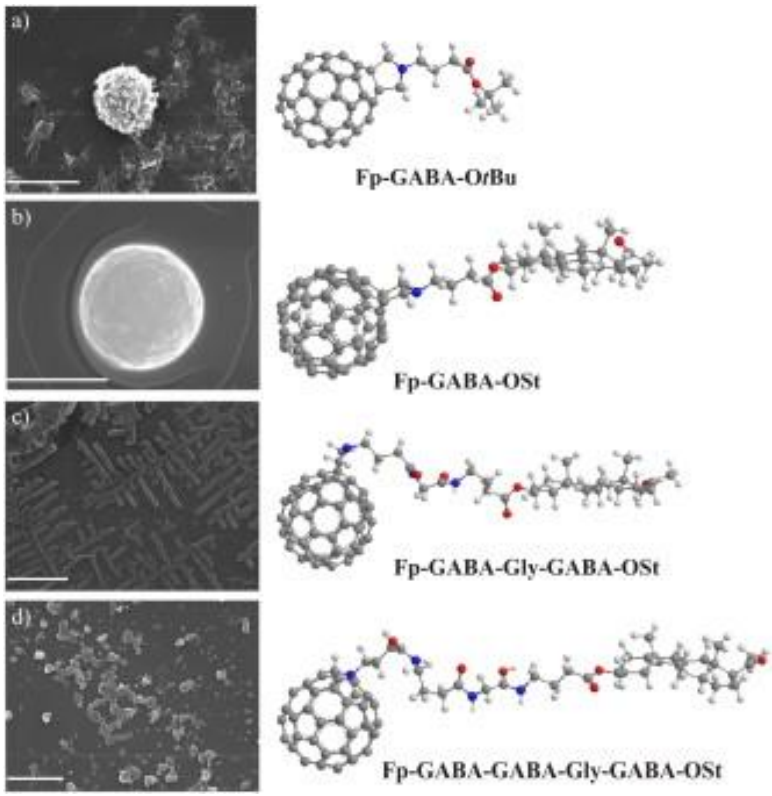
a)
b)
c)
d)
Fp-GABA-OtBu
Fp-GABA-OSt
Fp-GABA-Gly-GABA-OSt
Fp-GABA-GABA-Gly-GABA-OSt

Fig. 12.

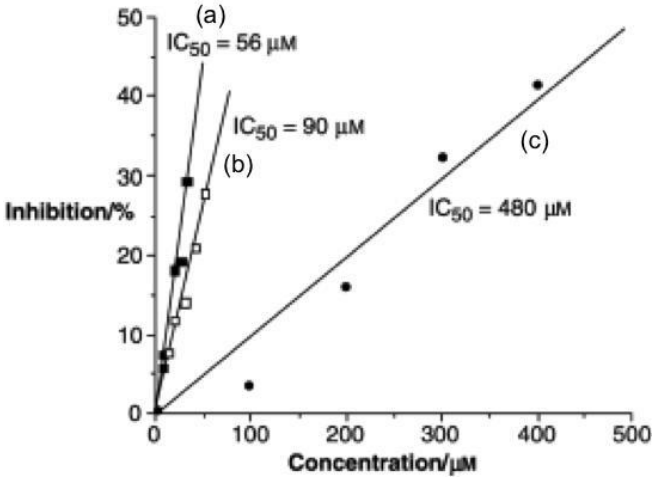
(a)
IC50 = 56 μM
IC50 = 90 μM
(b)
(c)
IC50 = 480 μM
Inhibition/%
Concentration/μM
0
10
20
30
40
50
0
100
200
300
400
500

Fig. 13.

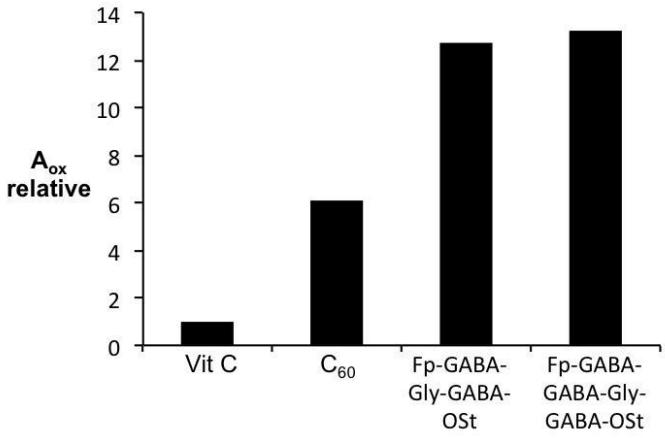
14
12
10
8
6
4
2
0
A_{ox} relative
Vit C
C_{60}
Fp-GABA-Gly-GABA-OSt
Fp-GABA-GABA-Gly-GABA-OSt

Fig. 14.

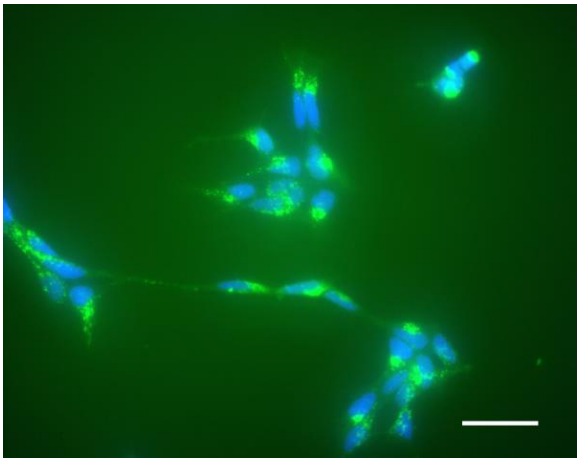

Fig. 15.

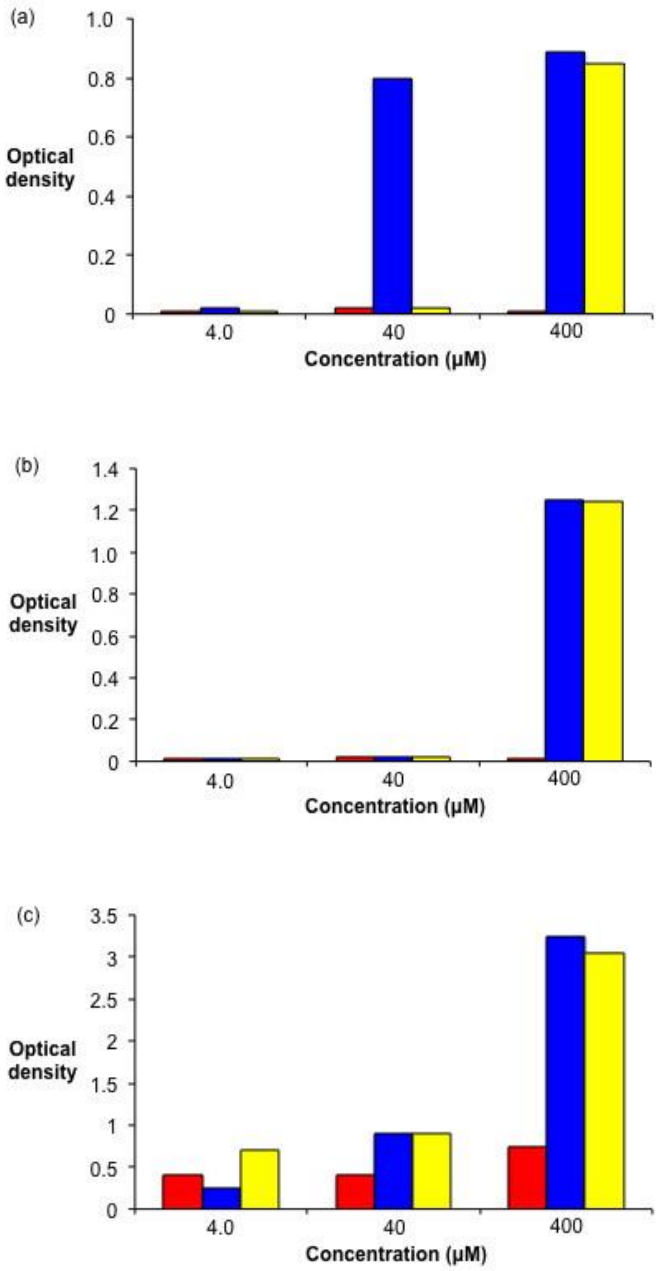
(a)
1.0
0.8
0.6
0.4
0.2
0
Optical density
4.0
40
400
Concentration (μM)
(b)
1.4
1.2
1.0
0.8
0.6
0.4
0.2
0
Optical density
4.0
40
400
Concentration (μM)
(c)
3.5
3
2.5
2
1.5
1
0.5
0
Optical density
4.0
40
400
Concentration (μM)

Fig. 16.

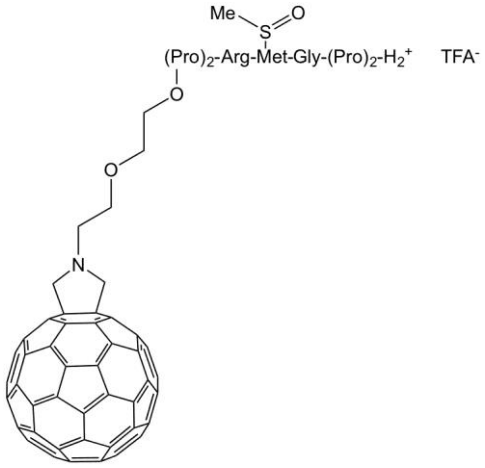

Fig. 17.

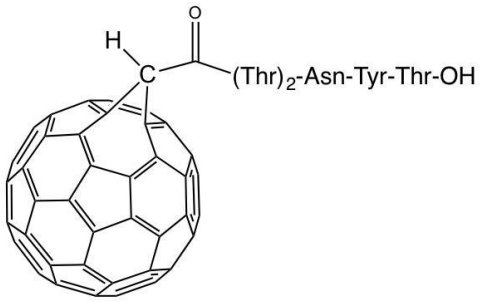

Fig. 18.

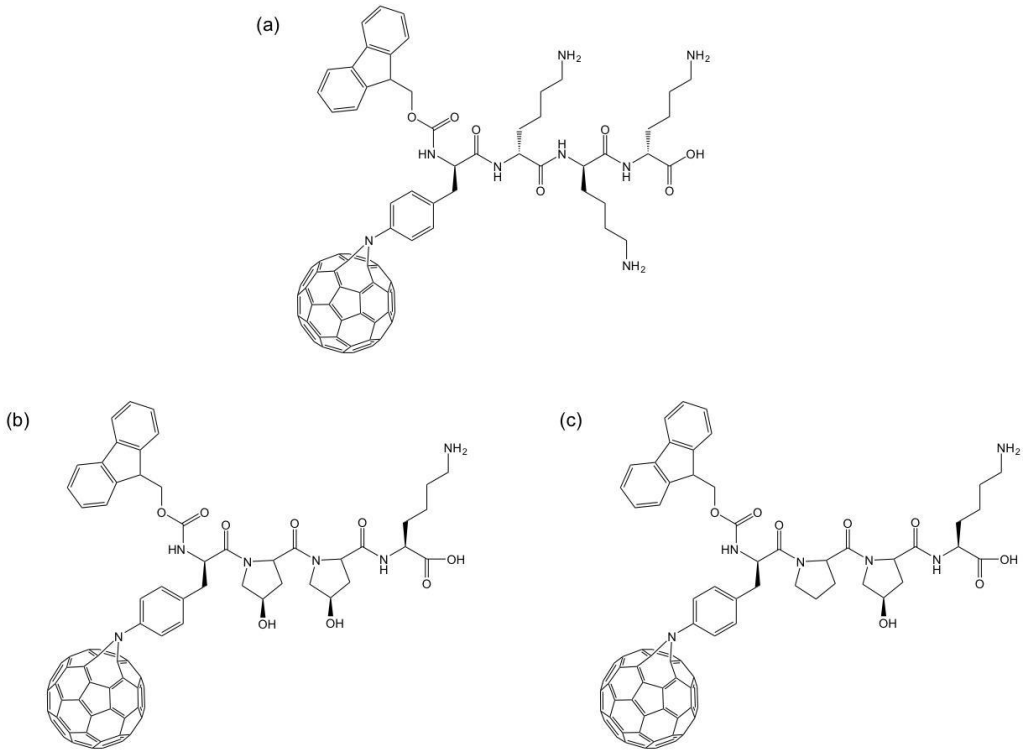

Fig. 19.

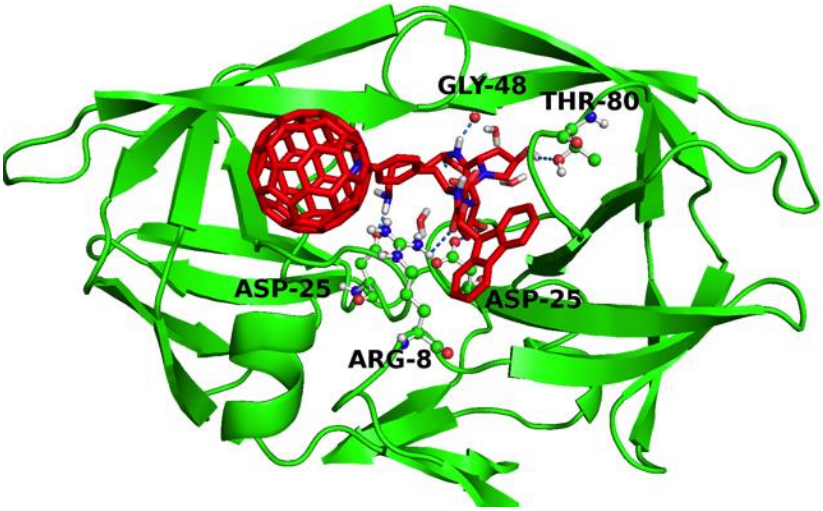

Fig. 20.